

Source detection via multi-label classification

Jayakrishnan Vijayamohanam, Arjun Gupta, Oameed Noakoasteen, Sotirios Goudos and Christos Christodoulou

Abstract—Radio source detection through conventional algorithms has been unreliable when trying to solve for large number of sources in the presence of low SINR and less number of snapshots. We address this by reformulating source detection as a multi-class classification problem solved using deep learning frameworks. Incoming waveforms are sampled using a centrosymmetric linear array with omni-directional elements and the normalized upper triangle of the autocorrelation matrix is extracted as the input feature to a modified convolutional neural network with uni-dimensional filters, trained to detect the sources in the presence of both uncorrelated and correlated signals. Two detection algorithms are introduced and referred to as CNNdetector and RadioNet, and subsequently benchmarked against the conventional source detection algorithms. By including pre-processing in forward backward spatial smoothing, RadioNet can also resolve the number of uncorrelated sources in the presence of correlated paths. Finally, the algorithms are stress tested under challenging operational conditions and extensive evaluations are presented showing the efficacy and contributions of the introduced predictive models.

Index Terms—Array Signal Processing, Multi-label Classification, ResNet, CNN, Direction of Arrival, Residual Learning, Signal Source Detection, Statistical Signal Processing

I. INTRODUCTION

RADIO events surround the world around us. We live in an increasingly connected environment fueled by hand held devices, household appliances, autonomous vehicles, and wearable devices; the ease of connectivity provided by multi-input multi-output (MIMO) systems and fast data rates of modern communication protocols. As a result, radio source detection has received significant attention over the years [1]–[5], and made its way into applications across various domains of science and engineering [2], [6]–[10]. High resolution direction of arrival (DoA) estimation algorithms such as MuSiC, root-MuSiC, ESPRIT and several others including non-parametric machine learning and deep learning methods require the knowledge of the number of sources to compute a viable localization estimation [1], [2], [11]–[14]. Maximum likelihood estimation (MLE) using a Gaussian assumption is considered the optimal solution to estimate the number of sources [2], [15], [16]. However, MLE is computationally expensive and is not a viable solution for real-time source detection. The conventional approach for estimating the number of sources is to apply information theoretic criterion like the minimum description length (MDL) or Akaike information

criterion (AIC) [17]–[19]. However, these approaches suffer degradation in detection performance in the presence of low Signal to Interference plus Noise Ratio (SINR), fewer number of samples, and an increasing number of sources to resolve [20]. Eigen methods involving the Eigen value decomposition (EVD) of the autocorrelation matrix have also been employed to estimate the number of sources with good success [21].

More recently, deep neural network (DNN) architectures such as auto-encoder and long short-term memory (LSTM) have been shown to perform source localization with good accuracy [1], [4], [14], [22], [23]. DNN based approaches have also been implemented to estimate source detection from the sampled waveform [24]–[28]. Some of the early works include vanilla networks capable of detecting the presence of no more than 4 source signals [24], [25]. In [26], a convolutional neural network (CNN) was trained to predict the number of sources by feeding it raw signal waveforms. This approach ignores the possibility of the autocorrelation being rank deficient, directly affecting the detection performance [29]. This drawback was resolved in [27], where a neural network was trained by feeding the Eigen vectors obtained from the autocorrelation as the input. This approach improved generalization and the overall detection performance of the algorithm. This model was also able to resolve correlated sources by performing forward backward spatial smoothing (FBSS) on the autocorrelation matrix [29]. However, computing the EVD can add additional computational complexity which can be avoided [1], [3].

In this paper, we introduce CNN based frameworks to detect the number of sources without the need to compute EVD. Furthermore, we introduce residual layers to improve on the performance over vanilla CNNs. Instead of computing the EVD, we extract the upper triangular elements of the autocorrelation matrix as the input feature. Note that the autocorrelation is a symmetric matrix and this reduction preserves all the spatial-temporal cues obtained from the waveform [1], [30]. We proceed to stress test the methods and frameworks in the presence of both uncorrelated and correlated sources to find the performance threshold for the algorithms. The major contributions of this paper are summarized below:

1. We introduce a novel detection framework and evaluate the models up to the operational threshold of $L - 1$ sources present in the sampled waveform, with L being the number of elements in the array. Literature pertaining to solving this problem considers only the presence of less than or equal to four or five sources to resolve [24]–[28].
2. Comprehensive detection analysis is done by studying the sensitivity of the algorithms to a varying number of correlated and non-correlated sources. Section IV goes over experiments investigating the interactions between the number of correlated and uncorrelated sources and their effects on the detection

This work has been submitted to the IEEE-OJSP for possible publication. Copyright may be transferred without notice, after which this version may no longer be accessible. Jayakrishnan Vijayamohanam (jayakrishnan@unm.edu), Arjun Gupta, Oameed Noakoasteen, and Christos Christodoulou are with the Department of Electrical and Computer Engineering, University of New Mexico, Albuquerque, NM, 87131 USA. Sotirios Goudos is with Department of Physics, Aristotle University of Thessaloniki, 54124 Greece

probability.

The rest of the paper is organized in four parts. Section II describes the problem formulation in terms of the signal model and feature extraction. Section III introduces the CNNDetector and its strength and weakness are investigated to discover the shortcomings of the CNNDetector. In Section IV, we introduce residual learning in the form of RadioNet to improve on CNNDetector. We demonstrate the improvement provided by RadioNet and show the improvement in generalization provided over existing models and methods. Finally, the results are concluded in Section V.

II. PROBLEM FORMULATION

A. Signal Model

We begin the investigation around the ideal case of source detection in the absence of correlated or coherent sources and then extend to the more complex scenario of source detection in the presence of coherent sources. We consider a centro-symmetric linear array of L identical antennas placed along an axis with the center of the array coinciding with the origin of the co-ordinate system. The aperture of this array is illuminated by M non-coherent signals, N number of snapshots are captured, and the source location θ_{M_i} is chosen arbitrarily from $-60^\circ \leq \theta_{M_i} \leq 60^\circ$. The inter elemental spacing within the array is denoted by \tilde{d}_i . The complex envelope model of the received signal $\mathbf{X}(t) \in \mathbb{C}^{L \times N}$ can be modeled as,

$$\mathbf{X}(t) = \mathbf{A}(\theta) \mathbf{S}(t) + \mathbf{n}(t) \quad (1)$$

where $\mathbf{A}(\theta) = [\mathbf{a}(\theta_1), \mathbf{a}(\theta_2), \dots, \mathbf{a}(\theta_M)] \in \mathbb{C}^{L \times M}$ is the array manifold matrix, which contains steering vectors of the form

$$\mathbf{a}(\theta_m) = [1, e^{j2\pi \frac{\tilde{d}_1}{\lambda} \sin(\theta_2)}, \dots, e^{j2\pi \frac{\tilde{d}_{L-1}}{\lambda} \sin(\theta_M)}]^T \quad (2)$$

$\mathbf{S}(t) \in \mathbb{C}^{M \times N}$ consists of the independent signal vectors which can be denoted by $\mathbf{s}_1, \dots, \mathbf{s}_M$. These independent signals are generated by applying Quadrature Phase Shift Keying (QPSK) modulation to a random bit sequence. $\mathbf{n}(t) \in \mathbb{C}^{L \times 1}$ is an additive white Gaussian noise (AWGN) vector [31]. λ is the signal wavelength.

This assumption of uncorrelated sources however is often too simplistic when modelling RF environments in dense urban areas. To accurately model such environments we need to introduce a varying number of correlated or coherent sources in the mix. If one of the original transmitted signal can be denoted by $s_1(t)$, then the k th coherent signal of $s_1(t)$ can be written as,

$$\mathbf{s}_k(t) = \rho_k e^{j\phi_k} \mathbf{s}_1(t) \quad (3)$$

where ρ_k is the amplitude fading factor and ϕ_k is the phase change caused due to multi-path fading. The received signal $\mathbf{S}(t)$ can be modelled as a collection of both independent and correlated signals closely replicating the modern communication environment. $\mathbf{S}(t) \in \mathbb{C}^{M \times N}$ contains both the zero mean independent signals and the correlated signals generated using 3. The presence of correlated signals would result in the matrix being rank-deficient [29]. To avoid this, we use FBSS to smooth the autocorrelation before extracting the

feature vectors. To compute FBSS, the array is divided into K overlapped subarrays with $K = L - L_0 + 1$, L_0 being the dimension of each sub-array. The smoothed autocorrelation matrix is given by,

$$\mathbf{R}_{\text{fb}} = \frac{1}{2K} \sum_{k=1}^K (\mathbf{R}_{\text{ff}}^{(k)} + \mathbf{R}_{\text{bb}}^{(k)}) \quad (4)$$

where, $\mathbf{R}_{\text{ff}}^{(k)}$ and $\mathbf{R}_{\text{bb}}^{(k)}$ are the forward and backward autocorrelation matrices constructed from the k th subarray and \mathbf{R}_{fb} is the spatially smoothed autocorrelation matrix.

B. Feature Extraction

Due to the symmetry of the autocorrelation matrix, extracting the upper triangular elements along with the diagonals should provide sufficient information for learning algorithms [1]. For each sensor, the real and imaginary part is separated, and then normalized to obtain a column vector of dimension, $(L * (L + 1))$. This way the upper-triangle of the computed \mathbf{R}_{xx} , or \mathbf{R}_{fb} in the case of correlated signals, becomes the input feature for the learning algorithms. Since we train the model using synthetic data generated by realistic simulations, we control the number of signals in sampled waveform for a given time instance which becomes the ground truth or the target variable [1].

III. DETECTION FRAMEWORK I

We begin with the premise that the information on the number of sources is contained within the autocorrelation matrix obtained from the sampled waveform [1], [2]. We make use of the observation that a well designed neural network with substantial depth should be able to learn the mapping from the information present in the autocorrelation to the number of sources present in the sampled waveform as demonstrated in [32]–[34].

In this section we propose a detection framework developed with convolutional neural nets (CNN) as the core learning unit. CNNs are a class of neural network architecture which make use of filters to extract underlying information within the data and are capable of extracting highly abstract features from structured data such as images [1], [35]–[37]. As such, they have been adopted and reformulated to perform various computer vision objectives such as object detection, localization and semantic segmentation. We start the detection architecture design with a rather simple stacked CNN framework referred to as the CNNDetector.

A. CNNDetector

The CNNDetector architecture is composed of stacks of convolutional layers, followed by a fully connected layer to generate the discrete outputs in the form of a one-hot encoded target vector. To account for the uni-dimensional feature vector obtained from feature extraction we employ 1D convolutions with uni-dimensional filters as visualized in Figure 1. The kernel size is kept constant at $[1 \times 3]$, and batch normalization is performed after each layer to normalize the contribution to a layer for every mini-batch [38]. Batch normalization achieves

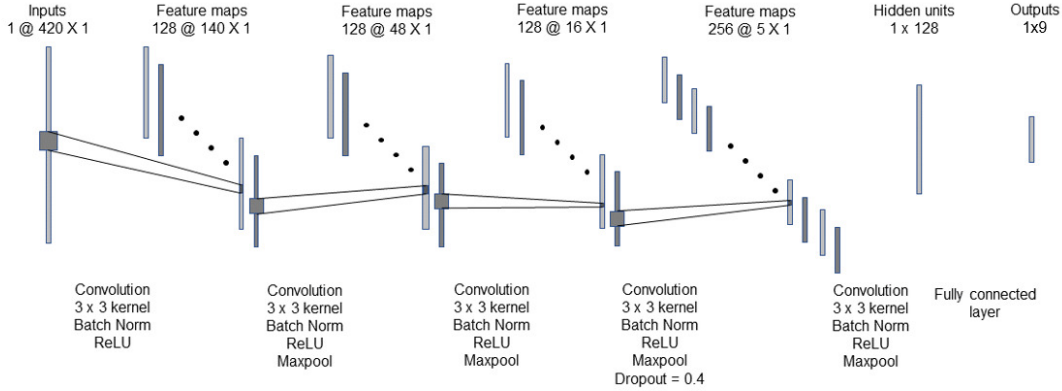


Fig. 1. Network architecture of the CNNDetector.

fixed distributions of inputs and prohibits internal covariate shift. Pooling is done in the last four convolutional layers. We optimize the number of layers along with the number of filters used in each layer. We found the 5 stacked CNN layers provides enough depth for detection without overfitting on the data. The number of filter size was 128, except in the fourth layer where it is increased to 256. The fourth convolutional layer also includes a dropout rate of 40% to facilitate generalization. The output layer was kept a constant at $[1 \times L - 1]$, L being the number of elements in the array. We minimize a categorical cross-entropy loss defined as,

$$\mathcal{L} = - \sum_{i=0}^{L-1} y_i \cdot \log(\tilde{y}_i) \quad (5)$$

here \tilde{y}_i is the i^{th} scalar value in the model output and y_i is the corresponding target value [39]. The categorical cross-entropy is a measure of the difference between the discrete distributions corresponding to each possible class in the problem. Minimizing the negative loss ensures that the loss becomes increasingly smaller as the distributions converge. The network parameters were initialized using Xavier initialization. This is done so that the variance remains the same across every layer [40]. Once the network is trained it is evaluated using the detection algorithm for uncorrelated sources presented in Algorithm 1.

B. Experiments and Evaluation

We evaluate the framework in the context of source detection in the presence of uncorrelated sources only. Since we extracted the features from the autocorrelation matrix, the theoretical maximum number of sources this approach can resolve is capped at $L - 1$. We use a 10 element array for the studies in this paper without any loss of generalization, the theories and methods can be readily extrapolated to arrays of any given size and shape. The data for training and testing the networks were generated using the equations introduced

Algorithm 1: Source number detection using CNNDetector

```

1: Require:  $\mathbf{X}$ ,  $L$ ,  $CNNDetector$ 
2: Outputs:  $y_{label}$ 
3:  $temp \in \mathbb{C}^{1 \times (L \cdot (L+1)/2)}$   $\leftarrow$  random temporary array
4:  $k, l = 1$ 
5:  $\mathbf{R}_{xx} = \mathbf{X} \cdot \mathbf{X}^H$ 
6: for  $i \in \{1, \dots, L\}$  do
7:   for  $j \in \{l, \dots, L\}$  do
8:      $temp[k] = \mathbf{R}_{xx}[i, j]$ 
9:      $k += 1$ 
10:  end for
11:   $l += 1$ 
12: end for
13:  $i = 1$ 
14: for  $j \in \{1, \dots, (L \times (L+1)/2)\}$  do
15:    $feature\ vector[i] = \Re(temp[j])$ 
16:    $i += 1$ 
17:    $feature\ vector[i] = \Im(temp[j])$ 
18:    $i += 1$ 
19: end for
20:  $y_{label} \leftarrow CNN\ detector(feature\ vector)$ 
21: return  $y_{label}$ 

```

in Section II. 110,000 frames were generated and further partitioned into 90,000 samples for training, 10,000 each for validation and test. Each frame is composed of 256 snapshots, which are used to compute the autocorrelation for a given frame. The test set is quarantined while the machine is trained on the training set and validated using the validation set repeatedly. Once the machine has achieved a saturation, the training is stopped and the test set is used to evaluate the model and generate the evaluation statistics. The number of sources to resolve is varied between 0 or no source present in the sampled waveform to 9 or the maximum detection capability

Class	CNNDetector		
	Precision	Recall	F1
Class 0	1	1	1
Class 1	1	1	1
Class 2	0.99	1	0.99
Class 3	0.97	0.99	0.98
Class 4	0.93	0.95	0.94
Class 5	0.89	0.91	0.90
Class 6	0.86	0.86	0.86
Class 7	0.79	0.79	0.79
Class 8	0.75	0.69	0.72
Class 9	0.80	0.82	0.81

TABLE I
PRECISION, RECALL AND F-1 SCORE OBTAINED FOR EXPERIMENT WITH
NON COHERENT SOURCES FOR DETECTION FRAMEWORK-I.

for a ten element array. The classification accuracy on the test set was found out to be 89%.

However, classification accuracy is not the ideal metric to evaluate a multi-class classification problem [35], [41]. To evaluate further, we compute and tabulate the precision, recall and f-1 score in Table I. Precision is formerly defined as the positive predicted value and recall is the percentage of true positives that were correctly classified. The f-1 score is the harmonic mean between these two values [42].

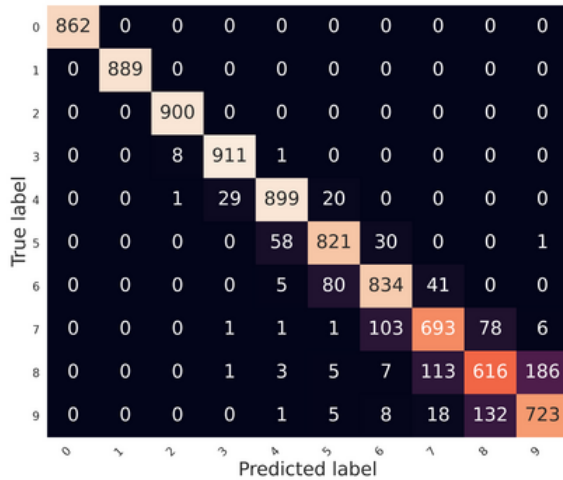


Fig. 2. Confusion matrix for CNNDetector. Rows in the table correspond to the True labels and columns are the predicted labels.

Finally, the performance of the framework on the test set is visualized using a confusion matrix in Figure 2. Each row in this matrix is the actual number of occurrence of each class in our test set, and each column is the respective classification by the algorithm [43]. In the confusion matrix we observe that the network accuracy of classification decreases as the number of sources increases. Samples with low number of sources (0-2) had none of the data miss-classified. In agreement with our precision and recall values, the classification error increases with an increasing number of sources to resolve. For a large presence such as with 8 sources, CNNDetector

correctly classifies only 616 out of 931 (66.16%) instances of the specific class in the test data. It fares slightly better with the class of 9 sources, where it improves its performance and classifies 723 out of 887 (81.5%) samples correctly. This can be explained by the reasoning that the extreme tail end of the distribution (maximum number of sources) is relatively more easy for mapping and thus the machine error is less as compared to 7 or 8 sources. This reasoning is also validated by the precision, recall and f-1 scores for each class. To the best of the authors knowledge, no other literature has reported the performance of detection for such high number of sources present in the sampled waveform [26], [27], hence it is not possible to draw a reference.

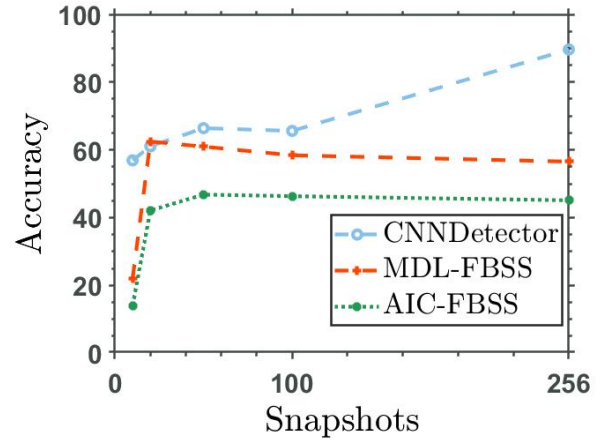


Fig. 4. Accuracy versus number of snapshots for 0-9 non correlated sources.

Next, we evaluate the CNNDetector from an operational point of view by varying SINR conditions. For any realistic scenarios, the SINR will vary and this does have a huge effect on any prediction model. We vary the SINR between $0dB$ to $20dB$ in four incremental steps and compare the detection performance to AIC and MDL. The corresponding accuracy for each of the discrete SINR thresholds probed in this research is presented in Figure 3. We observe that for 0

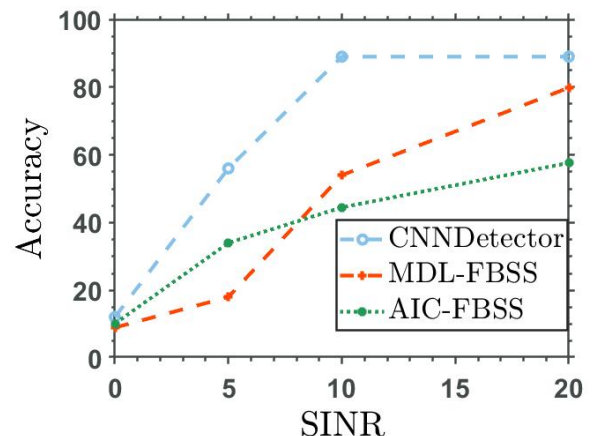


Fig. 3. Accuracy as a function of different SINR for the experiment involving 0-9 sources.

dB SINR, the accuracy of the CNNDetector is comparable to the conventional methods of MDL and AIC. But even with the slightest increase in signal power over the noise floor, the CNNDetector performs much better in term of accuracy than the conventional methods for a wide range of SINR until MDL catches up with CNNDetector when the SINR reaches 20 dB. The accuracy shown in Figure 3 is obtained by averaging the accuracy over all classes.

The frame size was fixed at 256 for the results presented above. However, we can perform detection with fewer number of snapshots in a frame, but the threshold is ambiguous at this point. To answer this research question we train different models by varying the frame size. We sweep the frame size between 10 and 256 for this experiment to analyze the change in performance for varying frame sizes. The corresponding accuracy for each of the discrete snapshot sizes investigated in this research is presented in Figure 4. The results are both surprising and intuitive. It turns out that the conventional methods such as MDL and AIC saturates at a relatively smaller number of snapshots around 20. The CNNDetector on the other hand is able to leverage the increasing number of snapshots available to it and keeps improving until we reach the max threshold of 256. There is no reason to believe that this behavior will not continue if we keep increasing the framesize.

IV. DETECTION FRAMEWORK II

A. RadioNet

The basic building block of RadioNet is a ResNet module introduced in [37]. Resnet models perform better than traditional CNNs because it is easier to optimize the residual mapping than to optimize the original complex desired mapping. The residual blocks form the backbone of the ResNet architecture and has shown to outperform conventional CNNs for a host of machine learning and computer vision applications [37], [44]. Increasing the number of layers result in very deep conventional networks which causes a saturation in learning at a threshold and the network with even greater depth becomes very difficult to optimize. ResNets solve this issue to a great extent by introducing residual blocks. Instead of learning the unreferenced function the network has an easier time learning the residual function with reference to the layer inputs. The output of the residual block can be written as,

$$\mathbf{y} = \mathcal{F}(\mathbf{x}) + \mathbf{x} \quad (6)$$

where, \mathbf{x} is the input to the block, and \mathbf{y} the output. The block is trained to learn $\mathcal{F}(\mathbf{x})$, which is less complex than the desired output $\mathcal{F}(\mathbf{x}) + \mathbf{x}$. Then at the output, an identity mapping is performed and the input is added to $\mathcal{F}(\mathbf{x})$. This forms the residual block. Stacking multiple such residual blocks were shown to decrease the training error faster while being easier to optimize as compared to a traditional CNN of same depth [37].

RadioNet is a ResNet34 model which consists of 16 residual blocks performing identity mapping with average pooling done before culminating into fully connected layers at the end. Small changes are made to the traditional Resnet34 architecture to accommodate our one-dimensional input data.

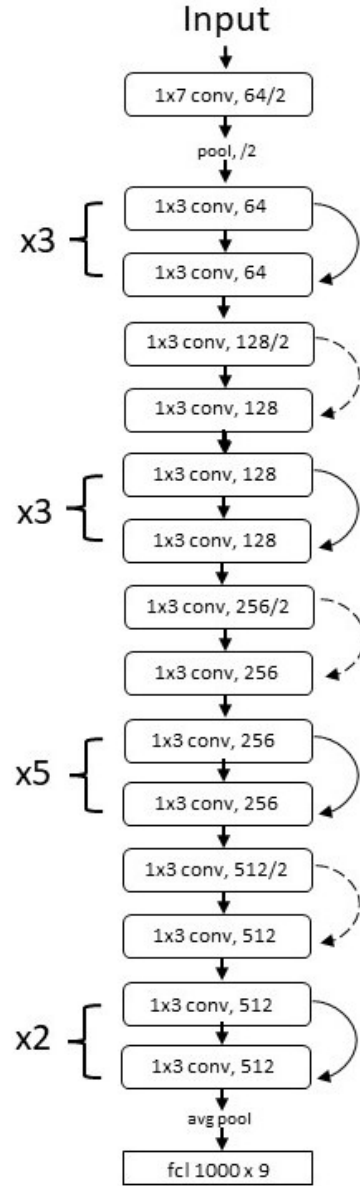


Fig. 5. Network architecture of RadioNet. The dotted arrows increase dimensions.

The size of the filter is $[1 \times 7]$ in the first layer, and then kept constant as $[1 \times 3]$. The number of filters vary from 64,128,256 and 512. These hyper-parameters are optimized using a grid search. The final architecture is as shown in Figure 5. We use the same categorical cross entropy loss function to train our network. The computed errors are backpropagated during training phase and used to update the weights with a learning rate of 0.0001. Stochastic Gradient Descent (SGD) is used to optimize the network parameters with a Nesterov momentum of value 0.9 in batches of size 64 [45]. Once the network is trained, it is tested for correlated sources as shown in Algorithm 2.

B. Experiments and Evaluation

For the second set of experiments, the dataset consisting of correlated sources was considered. In each frame, the number

Algorithm 2: Source number detection in the presence of coherent sources using RadioNet

```

1: Require:  $\mathbf{X}$ ,  $L$ ,  $RadioNet$ ,  $K$ 
2: Outputs:  $y_{label}$ 
3:  $temp \in \mathbb{C}^{1 \times (L \cdot (L+1)/2)} \leftarrow$  random temporary array
4:  $j=K$ 
5: for  $i \in \{1, \dots, k\}$  do
6:    $\mathbf{X}_f = \mathbf{X}[i : j, :]$ 
7:    $\mathbf{X}_b = \mathbf{X}[L - j + 1 : L - j + k, :]$ 
8:    $\mathbf{R}_f[i] = \mathbf{X}_f \cdot \mathbf{X}_f^H$ 
9:    $\mathbf{R}_b[i] = \mathbf{X}_b \cdot \mathbf{X}_b^H$ 
10:   $j+ = 1$ 
11: end for
12: for  $i \in \{1, \dots, k\}$  do
13:   $\mathbf{R}_{fb} = \mathbf{R}_f[i] + \mathbf{R}_b[i]$ 
14: end for
15:  $\mathbf{R}_{fb} = \mathbf{R}_{fb} / (2 \times K)$ 
16:  $l, m = 1$ 
17: for  $i \in \{1, \dots, L\}$  do
18:  for  $j \in \{l, \dots, L\}$  do
19:     $temp[m] = \mathbf{R}_{fb}[i, j]$ 
20:     $m += 1$ 
21:  end for
22:   $l += 1$ 
23: end for
24:  $j = 1$ 
25: for  $j \in \{1, \dots, (L \times (L + 1)/2)\}$  do
26:  feature vector[i] =  $\mathbb{R}(temp[j])$ 
27:   $i += 1$ 
28:  feature vector[i] =  $\mathbb{I}(temp[j])$ 
29:   $i += 1$ 
30: end for
31:  $y_{label} \leftarrow RadioNet(\text{feature vector})$ 
32: return  $y_{label}$ 

```

of non coherent sources is kept varying from 0 to 5 and the number of correlated sources is varied from 0 to 4. To perform FBSS on the sampled signals, the number of elements considered in the subarray is 5. The network is first trained on the first dataset for 10 epochs, and then later fed the second dataset consisting of correlated sources. In this experiment the CNNDetector was found to have an accuracy of only 56.7%. This was improved by RadioNet which obtained a validation accuracy of 82% after 100 epochs. The precision, recall and f-1 scores were also calculated as shown in Table II. We can see from this table that CNNDetector performs poorly in the presence of correlated sources, but RadioNet is still able to resolve upto 5 sources in the presence of correlated sources with a precision of 0.7.

We also study the effect SINR has on the model performance. Similar to the previous experiment, we run both our networks along with FBSS-MDL and FBSS-AIC for data collected of differing SINRs to compare the accuracy, as shown in Figure 6. We observe that both our deep learning based models consistently perform better than both MDL and AIC with FBSS. At higher SINR values RadioNet seems to

Class	CNNDetector			RadioNet		
	Precision	Recall	F1	Precision	Recall	F1
Class 0	1	1	1	1	1	1
Class 1	0.94	1	0.97	0.99	1	0.99
Class 2	0.60	0.86	0.71	0.99	1	0.99
Class 3	0.42	0.46	0.71	0.97	0.99	0.98
Class 4	0.36	0.07	0.12	0.63	0.65	0.64
Class 5	0.46	0.55	0.5	0.7	0.58	0.64

TABLE II
PRECISION, RECALL AND F-1 SCORE OBTAINED FOR EXPERIMENT WITH CORRELATED COHERENT SOURCES FOR CNNDETECTOR AND RADIONET.

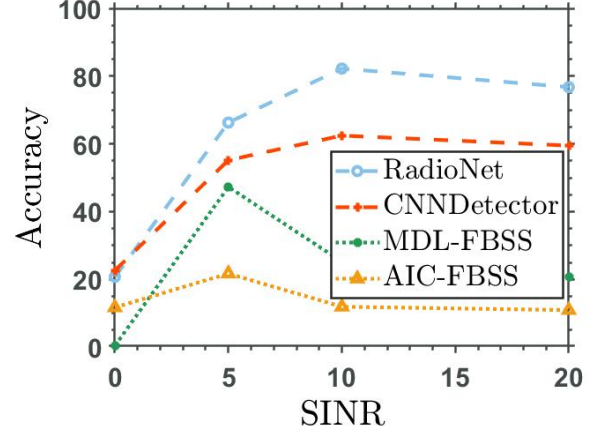


Fig. 6. Accuracy as a function of different SINR for the experiment involving 0-5 coherent sources.

perform far more better than MDL, AIC and CNNDetector, and hence seems to be the best choice for source detection.

Then we proceed to study the effect of the number of correlated sources affects the model performance in classifying each source. We create different datasets of varying number of coherent and correlated signals consisting of 3000 samples and test the trained models on it. We also use this dataset and test it on FBSS-MDL and FBSS-AIC. All these results obtained for each class are summarized in Figure 7. As seen in this plot, CNNDetector is the most suitable model while considering 1 or 2 non coherent signals. However its performance is surpassed by RadioNet when we increase the number of signals to 3. This can be understood by realizing that simpler networks are sufficient to solve problems of low complexity. The strength of resnet models is apparent only when we realize complex problems which traditional CNN models cannot solve. Both the deep learning solutions we propose have better accuracy than conventional techniques like MDL and AIC. We also see that the performance of our models tends to deteriorate if the number of correlated signals gets closer to the number of non coherent signals. Hence, it is shown that the proposed deep learning based models can perform source detection only when their number is less than the non-coherent signals. Finally the experiment was repeated with 1 million data points used for training. We also calculate the precision, recall and f-1 scores for each source in this experiment, as shown in Table III. This ten fold

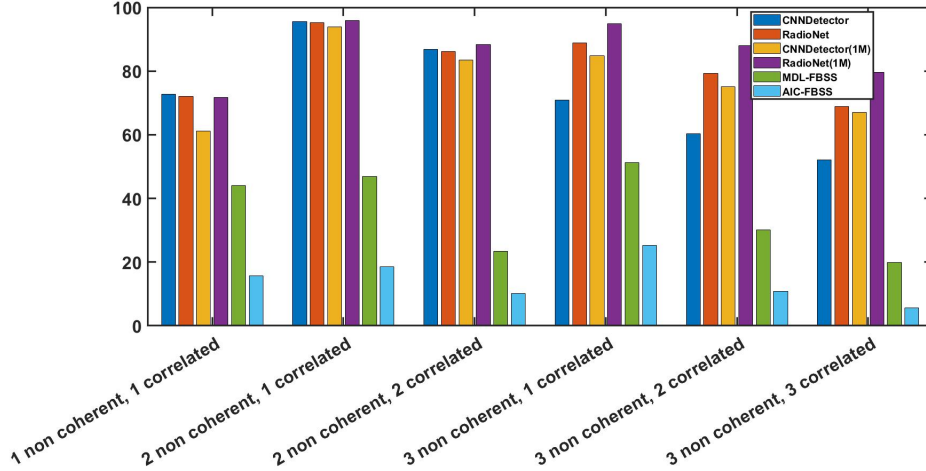


Fig. 7. Accuracy of CNNDetector and RadioNet as compared with MDL and AIC for varying number of correlated sources.

Number of sources	CNNDetector			RadioNet		
	Precision	Recall	F1	Precision	Recall	F1
0	1	1	1	1	1	1
1	0.99	1	0.99	0.99	0.99	0.99
2	0.85	0.90	0.88	0.90	0.94	0.92
3	0.75	0.79	0.77	0.83	0.84	0.84
4	0.70	0.68	0.69	0.79	0.72	0.75
5	0.74	0.68	0.71	0.77	0.79	0.78

TABLE III

PRECISION, RECALL AND F-1 SCORE OBTAINED FOR 0-5 CORRELATED SOURCES WITH CNNDETECTOR AND RADIO NET TRAINED ON ONE MILLION SAMPLES.

increase in the training dataset resulted in negligible changes in the CNNDetector performance. However RadioNet accuracy jumps up for each class. It attains an accuracy of 88% for 3 non coherent, 2 correlated case. Despite this improvement it only obtains an accuracy of 79.9% for 3 non coherent, 3 correlated case. Hence even RadioNet trained on one million samples is unsuccessful to resolve the number of sources when the number of coherent sources is equal to the number of correlated sources.

V. CONCLUSION

We introduced two modified CNN architectures referred to as the CNNDetector and RadioNet in this paper. The networks are trained to detect the number of sources sampled by an antenna array for a given time instance. We conduct extensive evaluation of the network with a large and diverse test set which can accurately identify for up to 9 sources for an array of 10 elements operating at a SINR as low as 5 dB. In a second set of experiments, RadioNet was shown to perform source detection even in the presence of correlated sources. The network performance was evaluated and RadioNet was shown to be better than all existing statistical and machine learning techniques.

VI. REPRODUCIBILITY

The datasets, code and results can be found at the Github repository dedicated to this work: https://github.com/jkrishnan95v/Signal_detector

ACKNOWLEDGMENT

The authors would like to thank The University of New Mexico Center for Advanced Research Computing, supported in part by the National Science Foundation, for providing the high-performance computing resources used in this work.

REFERENCES

- [1] M. Martínez-Ramón, A. Gupta, J. L. Rojo-Álvarez, and C. Christodoulou, *Machine Learning Applications in Electromagnetics and Antenna Array Processing*. Artech House, 2021.
- [2] H. L. Van Trees, *Detection, estimation, and modulation theory, Part I: optimum array processing*. New York: John Wiley & Sons, 2001.
- [3] A. Gupta, C. G. Christodoulou, J. L. Rojo-Álvarez, and M. Martínez-Ramón, "Gaussian processes for direction-of-arrival estimation with random arrays," *IEEE Antennas and Wireless Propagation Letters*, vol. 18, no. 11, pp. 2297–2300, 2019.
- [4] W. Liu, "Super resolution doa estimation based on deep neural network," *Scientific Reports*, vol. 10, 11 2020.
- [5] Z.-M. Liu, C. Zhang, and P. S. Yu, "Direction-of-arrival estimation based on deep neural networks with robustness to array imperfections," *IEEE Transactions on Antennas and Propagation*, vol. 66, no. 12, pp. 7315–7327, 2018.
- [6] B. F. Engin Tuncer, *Classical and Modern Direction-of-Arrival Estimation*. Elsevier Inc, 2009.

- [7] F. Viani, P. Rocca, G. Oliveri, D. Trinchero, and A. Massa, "Localization, tracking, and imaging of targets in wireless sensor networks: An invited review," *Radio Science*, vol. 46, no. 05, pp. 1–12, 2011.
- [8] D. Song, C.-Y. Kim, and J. Yi, "Simultaneous localization of multiple unknown and transient radio sources using a mobile robot," *IEEE Transactions on Robotics*, vol. 28, no. 3, pp. 668–680, 2012.
- [9] A. Gupta, M. Martínez-Ramón, C. G. Christodoulou, and J. Luis Rojo-Álvarez, "Bearing estimation with randomized linear arrays," in *2019 13th European Conference on Antennas and Propagation (EuCAP)*, 2019, pp. 1–3.
- [10] C. Uhl, M. Kern, M. Warmuth, and B. Seifert, "Subspace detection and blind source separation of multivariate signals by dynamical component analysis (dyca)," *IEEE Open Journal of Signal Processing*, vol. 1, pp. 230–241, 2020.
- [11] M. Carlin, P. Rocca, G. Oliveri, F. Viani, and A. Massa, "Directions-of-arrival estimation through bayesian compressive sensing strategies," *IEEE Transactions on Antennas and Propagation*, vol. 61, no. 7, pp. 3828–3838, 2013.
- [12] R. Schmidt, "Multiple emitter location and signal parameter estimation," *IEEE Transactions on Antennas and Propagation*, vol. 34, no. 3, pp. 276–280, 1986.
- [13] B. Rao and K. Hari, "Performance analysis of root-music," *IEEE Transactions on Acoustics, Speech, and Signal Processing*, vol. 37, no. 12, pp. 1939–1949, 1989.
- [14] A. Gupta, C. G. Christodoulou, M. Martínez-Ramón, and J. L. Rojo-Álvarez, "Deep neural nets for doa estimation with random arrays," in *2020 IEEE International Symposium on Antennas and Propagation and North American Radio Science Meeting*, 2020, pp. 2043–2044.
- [15] B. EFRON and D. V. HINKLEY, "Assessing the accuracy of the maximum likelihood estimator: Observed versus expected Fisher information," *Biometrika*, vol. 65, no. 3, pp. 457–483, 12 1978. [Online]. Available: <https://doi.org/10.1093/biomet/65.3.457>
- [16] J. Aldrich, "R.A. Fisher and the making of maximum likelihood 1912-1922," *Statistical Science*, vol. 12, no. 3, pp. 162 – 176, 1997. [Online]. Available: <https://doi.org/10.1214/ss/1030037906>
- [17] M. Wax and T. Kailath, "Detection of signals by information theoretic criteria," *IEEE Transactions on Acoustics, Speech, and Signal Processing*, vol. 33, no. 2, pp. 387–392, 1985.
- [18] K. Wong, Q.-T. Zhang, J. Reilly, and P. Yip, "On information theoretic criteria for determining the number of signals in high resolution array processing," *IEEE Transactions on Acoustics, Speech, and Signal Processing*, vol. 38, no. 11, pp. 1959–1971, 1990.
- [19] E. Fishler and H. Messer, "On the use of order statistics for improved detection of signals by the mdl criterion," *IEEE Transactions on Signal Processing*, vol. 48, no. 8, pp. 2242–2247, 2000.
- [20] E. Fishler, M. Grossmann, and H. Messer, "Detection of signals by information theoretic criteria: general asymptotic performance analysis," *IEEE Transactions on Signal Processing*, vol. 50, no. 5, pp. 1027–1036, 2002.
- [21] W. Chen, K. Wong, and J. Reilly, "Detection of the number of signals: a predicted eigen-threshold approach," *IEEE Transactions on Signal Processing*, vol. 39, no. 5, pp. 1088–1098, 1991.
- [22] A. Massa, D. Marcantonio, X. Chen, M. Li, and M. Salucci, "Dnns as applied to electromagnetics, antennas, and propagation—a review," *IEEE Antennas and Wireless Propagation Letters*, vol. 18, no. 11, pp. 2225–2229, 2019.
- [23] G. K. Papageorgiou and M. Sellathurai, "Direction-of-arrival estimation in the low-snr regime via a denoising autoencoder," in *2020 IEEE 21st International Workshop on Signal Processing Advances in Wireless Communications (SPAWC)*, 2020, pp. 1–5.
- [24] A. Barthelme, R. Wiesmayr, and W. Utschick, "Model order selection in doa scenarios via cross-entropy based machine learning techniques," *ICASSP 2020 - 2020 IEEE International Conference on Acoustics, Speech and Signal Processing (ICASSP)*, May 2020. [Online]. Available: <http://dx.doi.org/10.1109/ICASSP40776.2020.9053029>
- [25] O. Bialer, N. Garnett, and T. Tirer, "Performance advantages of deep neural networks for angle of arrival estimation," in *ICASSP 2019 - 2019 IEEE International Conference on Acoustics, Speech and Signal Processing (ICASSP)*, 2019, pp. 3907–3911.
- [26] W. Hu, R. Liu, X. Lin, Y. Li, X. Zhou, and X. He, "A deep learning method to estimate independent source number," in *2017 4th International Conference on Systems and Informatics (ICSAI)*, 2017, pp. 1055–1059.
- [27] Y. Yang, F. Gao, C. Qian, and G. Liao, "Model-aided deep neural network for source number detection," *IEEE Signal Processing Letters*, vol. 27, pp. 91–95, 2020.
- [28] A. Barthelme and W. Utschick, "A machine learning approach to doa estimation and model order selection for antenna arrays with subarray sampling," *IEEE Trans. Signal Process.*, vol. 69, pp. 3075–3087, 2021.
- [29] S. Pillai and B. Kwon, "Forward/backward spatial smoothing techniques for coherent signal identification," *IEEE Transactions on Acoustics, Speech, and Signal Processing*, vol. 37, no. 1, pp. 8–15, 1989.
- [30] C. Christodoulou and M. Georgiopoulos, *Applications of Neural Networks in Electromagnetics*, 1st ed. USA: Artech House, Inc., 2000.
- [31] A. Gupta, C. G. Christodoulou, J. L. Rojo-Álvarez, and M. Martínez-Ramón, "Gaussian processes for direction-of-arrival estimation with random arrays," *IEEE Antennas and Wireless Propagation Letters*, vol. 18, no. 11, pp. 2297–2300, 2019.
- [32] A. El Zooghby, C. Christodoulou, and M. Georgiopoulos, "A neural network-based smart antenna for multiple source tracking," *IEEE Transactions on Antennas and Propagation*, vol. 48, no. 5, pp. 768–776, 2000.
- [33] J. Vijayamohan, A. Gupta, O. Noakoosteen, and C. Christodoulou, "Convolutional neural networks for radio source detection," in *2021 IEEE International Symposium on Antennas and Propagation and USNC-URSI Radio Science Meeting (APS/URSI)*, 2021, pp. 1491–1492.
- [34] J. Vijayamohan, A. Gupta, S. Goudos, and C. Christodoulou, "Detecting coherent sources with deep learning," in *2022 IEEE USNC-URSI Radio Science Meeting (Joint with AP-S Symposium)*, 2022, pp. 98–99.
- [35] I. Goodfellow, Y. Bengio, and A. Courville, *Deep Learning*. MIT Press, 2016, <http://www.deeplearningbook.org>.
- [36] A. Krizhevsky, I. Sutskever, and G. E. Hinton, "Imagenet classification with deep convolutional neural networks," in *Advances in Neural Information Processing Systems*, F. Pereira, C. J. C. Burges, L. Bottou, and K. Q. Weinberger, Eds., vol. 25. Curran Associates, Inc., 2012. [Online]. Available: <https://proceedings.neurips.cc/paper/2012/file/c399862d3b9d6b76c8436e924a68c45b-Paper.pdf>
- [37] K. He, X. Zhang, S. Ren, and J. Sun, "Deep residual learning for image recognition," 2015.
- [38] S. Ioffe and C. Szegedy, "Batch normalization: Accelerating deep network training by reducing internal covariate shift," 2015. [Online]. Available: <https://arxiv.org/abs/1502.03167>
- [39] Z. Zhang and M. Sabuncu, "Generalized cross entropy loss for training deep neural networks with noisy labels," in *Advances in Neural Information Processing Systems*, S. Bengio, H. Wallach, H. Larochelle, K. Grauman, N. Cesa-Bianchi, and R. Garnett, Eds., vol. 31. Curran Associates, Inc., 2018. [Online]. Available: <https://proceedings.neurips.cc/paper/2018/file/f2925f97bc13ad2852a7a551802feea0-Paper.pdf>
- [40] X. Glorot and Y. Bengio, "Understanding the difficulty of training deep feedforward neural networks," in *Proceedings of the Thirteenth International Conference on Artificial Intelligence and Statistics*, ser. Proceedings of Machine Learning Research, Y. W. Teh and M. Titterton, Eds., vol. 9. Chia Laguna Resort, Sardinia, Italy: PMLR, 13–15 May 2010, pp. 249–256. [Online]. Available: <https://proceedings.mlr.press/v9/glorot10a.html>
- [41] K. P. Murphy, *Machine learning : a probabilistic perspective*. Cambridge, Mass. [u.a.]: MIT Press, 2013. [Online]. Available: https://www.amazon.com/Machine-Learning-Probabilistic-Perspective-Computation/dp/0262018020/ref=sr_1_2?ie=UTF8&qid=1336857747&sr=8-2
- [42] C. Goutte and E. Gaussier, "A probabilistic interpretation of precision, recall and f-score, with implication for evaluation," in *Advances in Information Retrieval*, D. E. Losada and J. M. Fernández-Luna, Eds. Berlin, Heidelberg: Springer Berlin Heidelberg, 2005, pp. 345–359.
- [43] T. Hastie, R. Tibshirani, and J. Friedman, *The Elements of Statistical Learning*, ser. Springer Series in Statistics. New York, NY, USA: Springer New York Inc., 2001.
- [44] Z. Wu, C. Shen, and A. van den Hengel, "Wider or deeper: Revisiting the resnet model for visual recognition," *Pattern Recognition*, vol. 90, pp. 119–133, 2019. [Online]. Available: <https://www.sciencedirect.com/science/article/pii/S0031320319300135>
- [45] H. Robbins, "A stochastic approximation method," *Annals of Mathematical Statistics*, vol. 22, pp. 400–407, 2007.